Journal of the European Ceramic Society 19 (1999) 363–372

PII: S0955-2219(98)00200-3
0955-2219/99/$—see front matter

Influence of the Precursors on the Formation and the Properties of $ZnFe_2O_4$

F. J. Guaita, H. Beltrán, E. Cordoncillo, J. B. Carda and P. Escribano*

Departamento de Química Inorgánica y Orgánica, Universitat Jaume I, 12080 Castellón, Spain

(Received 30 March 1998; revised version received 30 July 1998; accepted 6 August 1998)

Abstract

The phase $ZnFe_2O_4$, franklinite, with spinel structure, has been synthesised using solid-state reactions from the mechanically mixed powders of several precursor salts. However, this method requires a high-temperature treatment for some hours to homogenise the whole composition to obtain a single phase. In this paper $ZnFe_2O_4$ has been prepared by the ceramic method using different precursors of Fe and Zn. The spinel has also been prepared by a citrate route that allows to prepare a homogeneous single phase at lower temperature and shorter annealing time. The citrate method has let to obtain single phase of $ZnFe_2O_4$ at 600°C/2 h. In addition, this processing increases the inversion grade with respect to the ceramic ones obtained with the same precursor salts. The samples have been studied and characterised by means of differential thermal analysis (DTA), thermal gravimetric analysis (TGA), powder X-ray diffraction (XRD), Rietveld refinement method, Mössbauer spectroscopy, scanning electron microscopy (SEM), energy dispersion of X-ray spectrometry (EDX) and magnetic measurements. The inversion grade has been detected by means of Rietveld analyses and corroborated by magnetic measurements. © *1999 Published by Elsevier Science Limited. All rights reserved*

Keywords: spinels, ferrites, powders – chemical preparation, precursors – organic, $ZnFe_2O_4$.

1 Introduction

The spinels are an important class of compounds with a large variety of electronic properties: some spinels are superconductors with a relatively high transition temperature, others exhibit magnetic properties which make these systems interesting for magnetic storage devices and other technological applications.[1] Zinc ferrite ($ZnFe_2O_4$) has an almost normal spinel structure with a tetrahedral A-site occupied by Zn^{II} ions and octahedral B-site by Fe^{III} ions. Some authors[2] describe this material as an anomalous antiferromagnet with Néel temperature $T_N \approx 10\,K$ and paramagnetic Curie temperature $\theta_p \approx 0\,K$. The neutron powder diffraction at 4·2 K indicates a non-colinear antiferromagnetic ordering.[2] At high temperature, paramagnetic susceptibility obeys Curie–Weiss law with a constant considerably smaller than the one expected from the several spinel structure.[2] As it has been remarked by several authors,[2] the deviation of Curie constant from the expected value can be understood by assuming that a small amount of Fe^{III} ions would occupy tetrahedral A-sites and these ions would form clusters with Fe^{III} ions at octahedral B-sites due to the A–B interaction, which is much stronger than the B–B interaction.

Changes in cation distribution in this type of compounds confers special characteristics and properties, particularly, in magnetic properties. Some authors claim that partial inversion (in spinel structure) occurs depending on the procedure under which the compound is prepared.[1–4]. So, Schiessl *et al.*[1] used ceramic method and high temperatures (1200°C) to obtain single phase of the $ZnFe_2O_4$ spinel of good quality and with no inversion grade. But they obtained samples with small partial inversion by quenching from high temperatures. Contrasting, by a strict control of pH-value during coprecipitation reaction and subsequent heating at low temperatures (~100°C), Kamiyama *et al.*[2] produced very fine particles of $ZnFe_2O_4$ (tens of Å) that showed spinel structure with partial inversion. They varied the grade of inversion of these nanoparticled material through annealing the samples at several temperatures.

Furthermore, crystallite size has an important influence on the magnetical properties of such a compound as $ZnFe_2O_4$.[4,5] 'Anomalies' and differences from bulk magnetic properties of $ZnFe_2O_4$

*To whom correspondence should be addressed.

have been observed in ultrafine particles. Kamiyama,[2] and Sato *et al.*[4] have been investigating such magnetic properties in these materials and have found that the magnetisation decreases with increasing ultrafine particle size (crystallite size). This fact is interpreted by the idea that a Fe^{III} ion located at the A-site forms a cluster with its twelve nearest Fe^{III} neighbours at B-sites through coupling by the A-B interaction, which is much stronger than the B-B interaction. The number of these clusters would increase with decreasing ultrafine particle size because cation substitution is pronounced in small particles. Thus, the magnetisation increases with decreasing particle size (crystallite size).[4,5]

As it has been exposed above, cation distribution is quite important to be determined in order to understand the properties of this type of materials. However, the determination of the cation distribution in ferrites by the usual X-ray diffraction method is generally not easy because of the X-ray scattering ability of the component M, since Zn is close to that of element Fe.

In most of the cases, the synthesis of $ZnFe_2O_4$ is achieved by ceramic method, however, it is interesting to remark that in solid state reactions the extent of product formation is influenced by the area of interfacial contact and the diffusion processes through a product layer. The diffusion of reactants through a product layer depends on temperature, defect structure of product layers, grain boundary contacts, presence of impurities and effectiveness of phase boundary contacts.[6] Because of these problems above mentioned, the synthesis of a product by solid–solid reactions takes place with great difficulty and a high sintering temperature is indispensable to obtain dense ceramics. Moreover, the use of such high temperature leads to compositional and structural defects due to the evaporation of some constituents, such as Fe_2O_3. In case of the zinc ferrite, O'Neill[7] encountered that samples annealed at or above about 1000°C turned a darker colour, also found in $MgFe_2O_4$, and which is probably related to de development of some oxygen-deficient non-stoichiometry, e.g. according to the reaction:

$$6ZnFe_2O_4(\text{spinel}) \rightleftharpoons 4Fe_3O_4(\text{spinel}) + 6ZnO(\text{oxide or spinel}) + O_2 \uparrow \quad (1)$$

The darkening of colour is readily reversed by further annealing at lower temperature, and the material which has undergone such a cycle shows no difference in the final reticular parameter (a_o).[7] These facts could explain some differences in the characteristics of the 'same' material but prepared by several synthesis methods. For example, the ceramic method could not be appropriate to obtain a material with an equilibrium state difficult to reach or unstable.

As, in some cases, cation distribution can be modified by heat treatments, and in ceramic method high temperatures have to be reached, various chemical routes, mainly based on the hydrolytic precipitation of alkoxides, have been developed. The liquid-mix process (the so called Pechini process[8]) using citric acid is a method where there is a formation of a dense and rigid resin intermediate of citric acid and ethylene glycol by heating at a moderate temperature (150–250°C). The charring of the resin at 400°C breaks down the polymer and it is assumed that cations remain trapped in the char. Gajbhiye *et al.*[9] have studied the thermal decomposition of zinc–iron citrate precursor using thermal tecniques. It was found that decomposition in air was suitable for obtaining $ZnFe_2O_4$. Thermal decomposition involved several steps, in which adsorbed and coordinated water molecules were lost, the citrate groups lost water molecules to form metal aconitates and further decomposition occured in the temperature range 260–320°C. After that, hydrozincite and goethite were observed and decomposed into the oxides which reacted to form $ZnFe_2O_4$. In this paper and in order to overcome some of the problems of the synthesis of $ZnFe_2O_4$, we have studied the influences of some precursors for the Fe and Zn in the synthesis temperature by the ceramic method and once established the best precursors, we have synthesised this spinel following the Pechini method to reduce the temperature and time, in order to compare whether the method leads to an inversion grade different.

2 Experimental Procedure

Zinc ferrite ($ZnFe_2O_4$, franklinite, JCPDS 22-1012) was prepared in the polycrystalline form by both a solid state reaction (ceramic method, CM) and the varied form of Pechini method (PM). Table 1 shows the samples prepared and precursors employed, all of them of C.P. grade. The zinc oxide (ZnO) has been avoided as a precursor in an attempt

Table 1. Raw materials

Sample	*Iron precursor*	*Zinc precursor*
1CM	Fe_2O_3	$Zn(CH_3COO)_2{\cdot}2H_2O$
2CM	$Fe(NH_4)_2(SO_4)_2{\cdot}6H_2O$	$Zn(CH_3COO)_2{\cdot}2H_2O$
3CM	$Fe(NH_4)_2(SO_4)_2{\cdot}6H_2O$	$ZnSO_4{\cdot}7H_2O$
4CM	$FeSO_4{\cdot}7H_2O$	$ZnSO_4{\cdot}7H_2O$
5PM	$Fe(NH_4)_2(SO_4)_2{\cdot}6H_2O$	$ZnSO_4{\cdot}7H_2O$
6PM	$FeSO_4{\cdot}7H_2O$	$ZnSO_4{\cdot}7H_2O$

to reduce synthesis temperature, even in ceramic samples. In spite of using this oxide, we have decided to use dihydrated zinc acetate and heptahydrated zinc sulphate. The iron precursors employed have been the following ones: iron (III) oxide, Mohr salt and heptahydrated iron (II) sulphate.

In Fig. 1(a) and (b), the flow diagrams for the preparation of the samples by both methods are shown. In the ceramic method, samples were refined and homogenised in acetone in a planetary ball mill and finally dried. From the best results of X-ray diffraction (XRD) scans for ceramic compositions (3CM and 4CM), 5PM and 6PM samples were prepared following the Pechini method, using the same starting materials. In the Pechini method, first citric acid and ethylene glycol are mixed and then stirred at about 100°C until it becomes transparent. After that, cation solutions are added to the mixture of citric acid and ethylene glycol at a temperature of 100°C. This solution thus obtained is heated stirring up to about 140°C in order to promote the ester reaction between citric acid and ethylene glycol. As removing solvent, mixture concentrates and becomes highly viscous, and polymeric gelation occurs. The viscous polymeric product is heat-treated at about 350°C. The black powder thus obtained (precursor system), is calcined in air at about 450°C for 1 h. Our preparation attended the following steps: the quantity of anhydrous citric acid in molar ratio to cations 1:1 was first dissolved using the minimum amount of distilled water; zinc and iron precursors salts were separately dissolved in the same way. Then the three solutions were mixed at a temperature of 70°C. After homogenisation, ethylene glycol (1:1 molar ratio to cations) was poured into the reaction vessel. The solution was heated up to 100°C and polymeric gelation occurred by removing the solvent. The raw material thus obtained was later dried at 110°C for 2 days. The polymeric product was then heat-treated at 350°C for 1 h in order to remove the remained solvent and organics in an electrical furnace. After grinding of the resulting black mass, a precursor system was obtained. The subsequent heat-treatments led to an orange-brown powder in which single crystalline phase was detected.

2.1 Sample characterisation

In order to design the firing treatments, differential thermal analyses (DTA) and thermal gravimetric analyses (TGA) were performed in a Perkin–Elmer Model 1700 instrument at a heating rate of 10°C min^{-1} in air atmosphere. From the results of DTA/TGA and XRD analyses, dried samples were fired in air at 350, 500, 600, 700, 800, 900 and 1000°C with annealing times of 2 and 4 h in an electrical furnace CARBOLITE model at a heating rate of

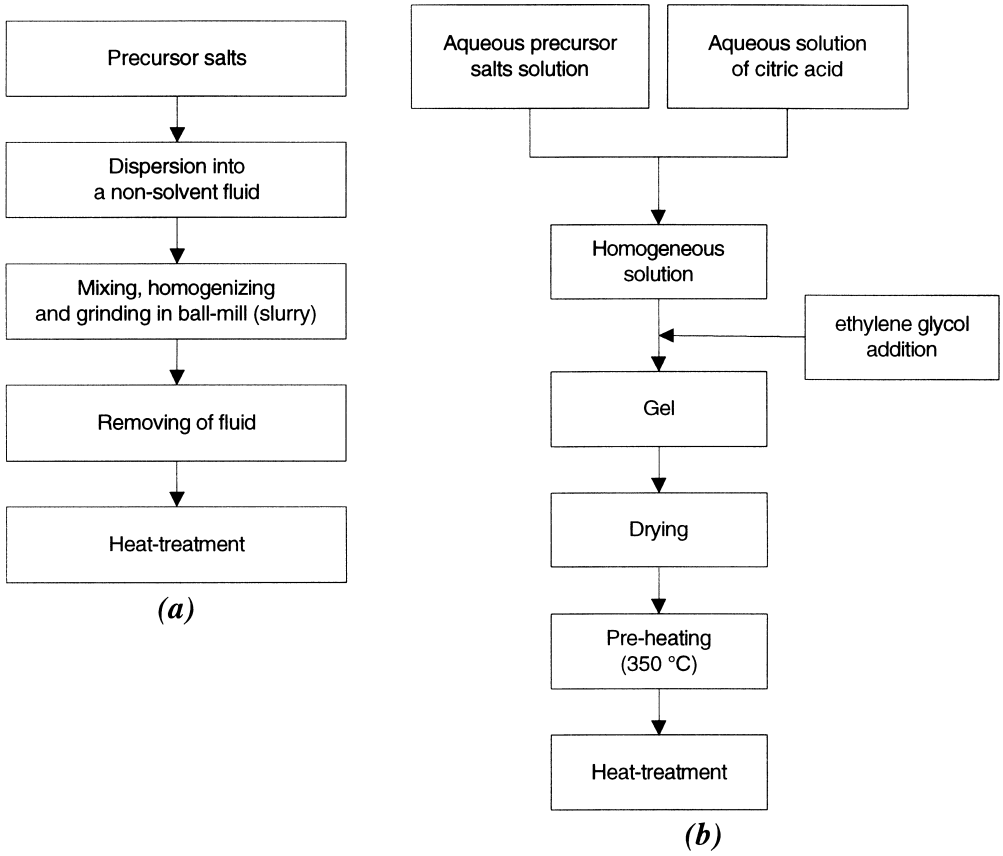

Fig. 1. (a) Ceramic processing flowchart; (b) Pechini processing flowchart.

10°C min^{-1}. After heat-treatment, samples showed orange-brown coloration.

Crystalline phase evolution of calcined powders was carried out with a Siemens D5000 diffractometer with Bragg-Brentano geometry using CuK_α radiation (40 kV, 20 mA, divergence slit = 1°; receiving slit = 1°; detection slit = 0·15°) scintillation detector and a secondary graphite monochromator. Intensities were collected by step-scanning from 20 to 70° (2θ) with a step size of 0·05° (2θ) and 1 s counting time each step. The goniometer was controlled by the Siemens Diffract Plus software, which makes the integration of the diffraction peaks.

The refinement of structure was carried out by using the FULLPROF program, developed by Rodríguez-Carvajal[10] from X-ray powder diffraction data obtained in following experimental conditions: 40 kV, 30 mA, divergence slit = 0·5°; receiving slit = 0·5°; detection slit = 0·15°; scanning

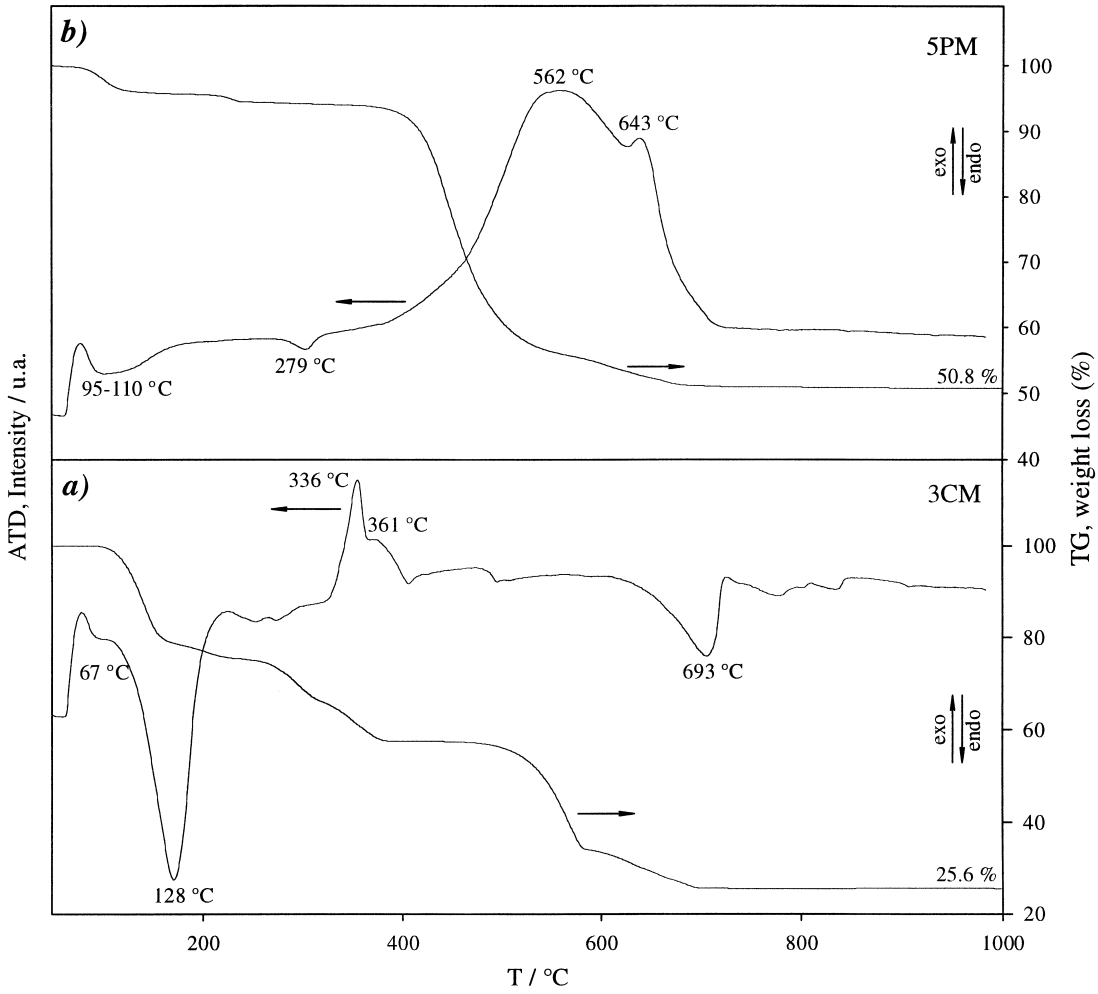

Fig. 2. DTA/TG analysis of samples: (a) 3CM; (b) 5PM.

Table 2. Evolution of crystalline phases detected by XRD

T(°C)	t_{anneal}	1CM	2CM	3CM	4CM	5PM	6PM
500	2 h	H(s), Z(m)	G(vw)	G(m)	G(m)	F(s), G(vw)	F(s), G(vw)
	4 h	H(s), Z(m)	SF(vw), G(vw)	G(m)	G(m)	F(s), H(w)	F(s), G(w), Z(vw)
600	2 h	H(s), Z(m)	H(m), SF(vw)	SF(s), G(m)	G(m), SF(m), H(w)	F(vs)	F(s), H(m), G(w)
	4 h	H(s), Z(m)	H(m), SF(vw)	SF(s), G(m)	H(m), G(m), SF(m)	F(vs)	F(s), H(m)
700	4 h	H(s), Z(w)	H(m), SF(vw)	H(s), SZ(m), SF(w)	H(s), SZ(m), SF(w), F(w)	F(vs)	F(s), H(w)
800	2 h	F(s), H(vw)	F(vs), H(vw)	F(vs), H(m)	F(s), H(vw)	F(vs)	F(vs)
	4 h	F(s), H(vw)	F(vs)	F(vs)	F(vs)	F(vs)	F(vs)
900	2 h	F(vs), H(vw)	F(vs)	F(vs)	F(vs)	F(vs)	F(vs)
	6 h	F(vs), H(vw)	F(vs)	F(vs)	F(vs)	F(vs)	F(vs)
1000	4 h	F(vs), H(vw)	F(vs)	F(vs)	F(vs)	F(vs)	F(vs)

Peak intensity: vs, very strong; s, strong; m, medium; w, weak; vw, very weak. Crystalline phases: F, $ZnFe_2O_4$ franklinite; G, $Zn_5O_4{\cdot}H_2O$ gunningite; H, α-Fe_2O_3 α-haematite; OX, Fe_2O_3 iron oxide; SE, $FeSO_4$ iron sulfate; SF, $Fe_2(SO_4)_3$ iron sulfate; SZ, $ZnSO_4$ zinc sulfate; Z, ZnO zincite.

range from 10 to 120°(2θ) with a step size of 0·02 °(2θ) and 9 s counting time each step. The structural model and initial structural parameters for $ZnFe_2O_4$ were taken as follows: space group Fd3m; zinc and iron atoms were in the Wyckoff 8a and 16d special position and O atoms in the 32e special positions. Diffraction profiles were modelled by using a pseudo-Voigt function that was corrected for peak asymmetry for angles less than 40°(2θ). The final refinement converged to give R_F and R_{Bragg}. The refined crystallographic parameters were: a scale factor; the lattice parameter, a_o; the oxygen positional parameter, *u*; the grade of inversion, x; and the overall isotropic displacement temperature factor, B.

Scanning electron micrographs of the samples were taken on a scanning electron microscope (SEM) Leica, Leo 440 model, equipped with a spectrometer of energy dispersion of X-ray (EDX) from Oxford instruments, using the following operational parameters: acceleration voltage 20 kV, measuring time 100 s, working distance 25 mm, counting rate 1·2 kcps. The samples for microstructural and microanalysis determinations were deposited in an aluminium holder and coated by graphite film.

Some of the samples were analyzed by Mössbauer spectroscopy at room temperature in a Wissenschaftliche Electronic Gmbk. The employed radiation source was $^{57}Co/Cr$ and the velocity scale was calibrated using the hyperfine spectra of a natural α-Fe foil, which also served as the isomer shift reference.

The magnetic susceptibility as a function of temperature and the hysteresis loop (at 5 K) of samples 3CM, 4CM, 5PM and 6PM fired at 900°C/6 h were recorded using a commercial SQUID magnetometer ($H_{max} = 5\ T$).

3 Results and Discussion

3.1 Thermal analyses

All the samples were studied by DTA and TGA and in Fig. 2 the results for samples 3CM and 5PM are shown: (a) ceramic route; (b) Pechini method. At ca 120°C there is weight loss in TGA (20%) for sample 3CM that can be related to that endothermic peak at 128°C in DTA. These changes correspond to the dehydration of Mohr salt and heptahydrated zinc sulphate. The profile of DTA analysis of sample 3CM also shows two exothermic peaks at 335 C and 360 C, which are associated to reactions with weight loss, possibly to the elimination of NH_4^+ ions from Mohr salt. The wide band centred at 693°C correspond to the decomposition and removal of sulphates.

Table 3. $ZnFe_2O_4$ powder XRD structural refinements using Rietveld method of 3 CM, 4 CM, 5 PM and 6 PM samples fired at 900°C/6 h

sample	a_o *(Å)*	x *(0–1)*	u	B *(Å²)*	R_{Bragg}	R_F
3	8·4401(1)	0·0000	0·2606(4)	0·487	2·65	2·58
4	8·4387(1)	0·0130	0·2607(3)	0·531	2·56	2·72
5	8·4417(1)	0·0228	0·2603(3)	0·695	3·09	2·95
6	8·4410(2)	0·0626	0·2608(6)	0·821	4·93	5·04

Theoretical value a_o = 8·4411 Å (JCPDS 22-1012).

Table 4. Positional and ocupational data in Rietveld refinements of 3 CM, 4 CM, 5 PM and 6 PM samples fired at 900°C/6 h

(a)sample: 3CM. a_o = 8·4401(1)Å					
Atom	*Position*	g*(0–1)*	x	y	z
	A-site				
Zn(1)	8a	0·9856	1/8	1/8	1/8
Fe(1)	8a	0·0000	1/8	1/8	1/8
	B-site				
Zn(2)	16d	0·0144	1/2	1/2	1/2
Fe(2)	16d	1·0000	1/2	1/2	1/2
O	32e	1·0000	0·2606(4)	0·2606(4)	0·2606(4)
(b) sample: 4CM. ao = 8.4388(1)Å					
	A-site				
Zn(1)	8a	0·9462	1/8	1/8	1/8
Fe(1)	8a	0·0259	1/8	1/8	1/8
	B-site				
Zn(2)	16d	0·0538	1/2	1/2	1/2
Fe(2)	16d	0·9741	1/2	1/2	1/2
O	32e	1·0000	0·2607(3)	0·2607(3)	0·2607(3)
(c) Sample: 5PM. a_o = 8·4417(1)Å					
	A-site				
Zn(1)	8a	0·9059	1/8	1/8	1/8
Fe(1)	8a	0·0455	1/8	1/8	1/8
	B-site				
Zn(2)	16d	0·0941	1/2	1/2	1/2
Fe(2)	16d	0·9545	1/2	1/2	1/2
O	32e	1·0000	0·2603(3)	0·2603(3)	0·2603(3)
(d) Sample: 6PM. a_o = 8·4410(2)Å					
	A-site				
Zn(1)	8a	0·7703	1/8	1/8	1/8
Fe(1)	8a	0·1252	1/8	1/8	1/8
	B-site				
Zn(2)	16d	0·2297	1/2	1/2	1/2
Fe(2)	16d	0·8748	1/2	1/2	1/2
O	32e	1·0000	0·2608(6)	0·2608(6)	0·2608(6)

Table 5. Inversion grade and FWHM values from Rietveld refinements of 3 CM, 4 CM, 5 PM and 6 PM samples fired at 900°C/6 h

sample	a_o *(Å)*	x,*(0–1)*	$FWHM_{aver}$	$FWHM_{311}$
3CM	8·4401(1)	0·0000	0·1219	0·137
4CM	8·4388(1)	0·0130	0·1461	0·141
5PM	8·4417(1)	0·0228	0·1343	0·146
6PM	8·4410(2)	0·0626	0·1694	0·162

The two endothermic bands in DTA analysis of 5PM sample (100 and 280°C) are associated to drying processes and removing of occluded water. The large band centred at 560°C and a sharper peak at 640°C could correspond to the combustion of organic material present. In DTA of 5PM sample the decomposition of sulphates does not appear in the same way as in 3CM sample (693°C). This

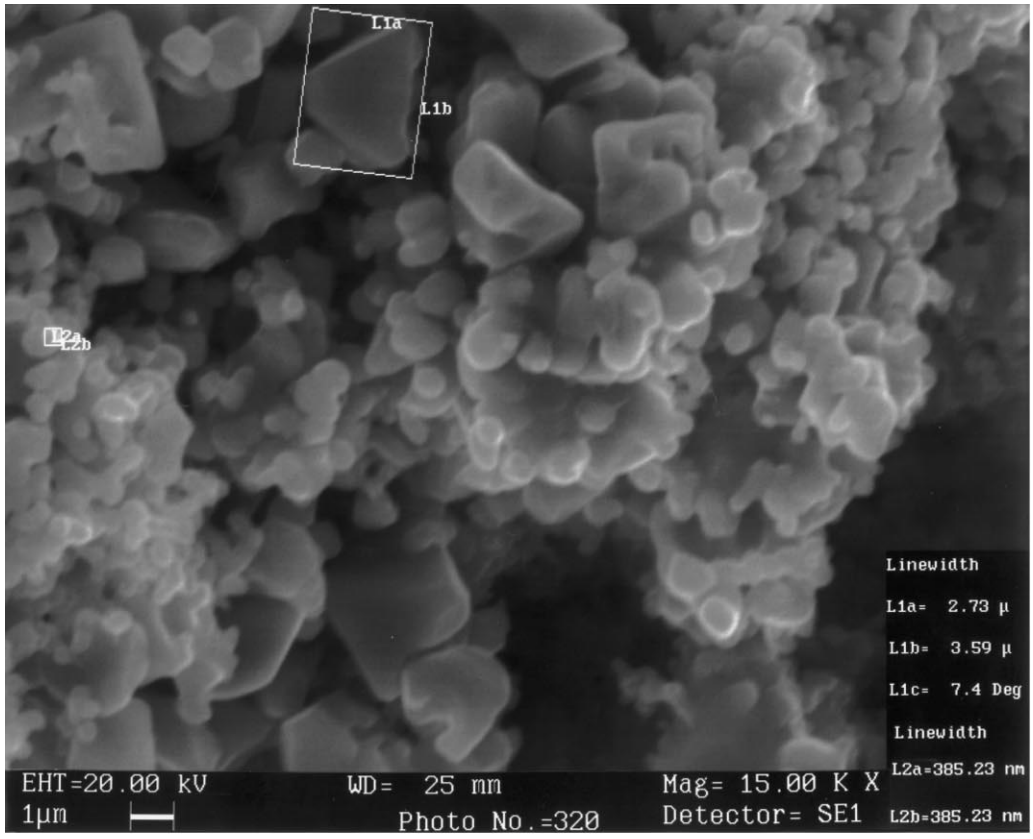

(a)

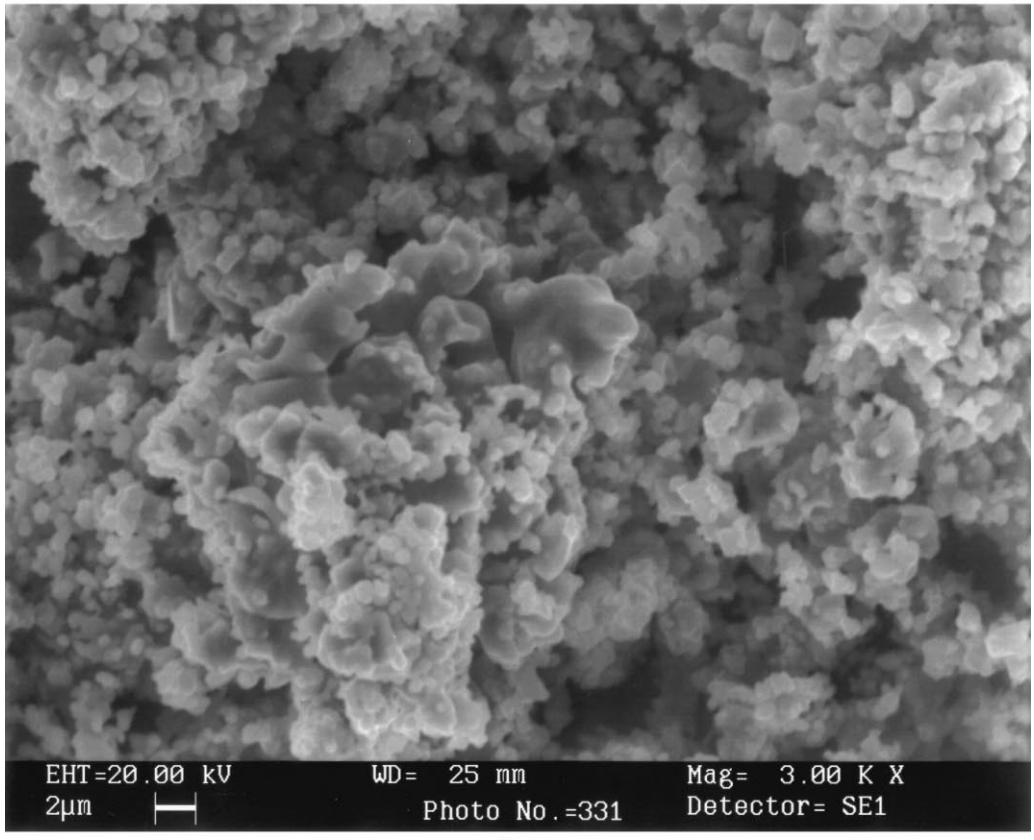

(b)

Fig. 3. Micrographs of (a) 4CM and (b) 6PM samples fired at 900°C/6 h.

fact could be associated to the polymeric product formed in the Pechini method.

In all samples the final powders obtained from DTA/TGA, were analysed by XRD and the results indicated that only the 1CM sample did not show a $ZnFe_2O_4$ as a single phase.

3.2 XRD analyses

Table 2, shows the evolution of crystalline phases of samples prepared by both methods. As it can be observed from this table, in ceramic route preparation, the samples 2CM, 3CM and 4CM exhibit franklinite peaks after firing at 800°C/2 h, but only as single phase after firing for 4 h at 800°C. Meanwhile, the 5PM sample, synthesised by the Pechini method, gave single phase of $ZnFe_2O_4$ at 600°C/2 h. In the 6PM sample, the $ZnFe_2O_4$ as single phase is obtained at 800°C/2 h. From these results it can be inferred that by this Pechini method $ZnFe_2O_4$ can be obtained at lower temperatures and times than in ceramic route, and the best precursor for Fe is Mohr salt.

From XRD results and in order to improve the development of $ZnFe_2O_4$ phase and its crystallinity, the samples for next characterisation were fired at 900°C/6 h.

3.3 Structure refinement (Rietveld method)

The cell parameters obtained from Rietveld analysis of samples fired at 900°C/6 h, are shown in Table 3. Data of reticular parameters are in good agreement with those of JCPDS 22-1012 (8·4411 Å), and are very similar in all samples.

In order to prove the influence of the methods and precursors employed in the inversion grade of $ZnFe_2O_4$, we have adjusted the experimental XRD data by using Rietveld method, with both Fe^{III} and Zn^{II} in octahedral and tetrahedral positions. The summarised results of XRD structural refinements shown in Tables 3–5 indicate an small inversion grade of the spinel for samples 4CM, 5PM and 6PM with values of 1·3, 2·3 and 6·3% respectively. In Table 5, values of FWHM for average and FWHM for 311 reflections are summarised. These values can be related to the crystallite size through the Scherrer's formula.

$$D = \frac{k\lambda}{B\cos\theta} \qquad (2)$$

where,
D: crystallite size in Å.
k: shape factor (usually 0·9–1).
λ: X-ray wave length in (Å), 1·54056 Å.
$B^2 = B_M{}^2 - B_P{}^2$; B_M: FWHM of the peak in rad; B_P: FWHM of the XRD peak in rad.
θ: Bragg angle in degrees.

According to such formula, 6PM sample shows the smallest crystallite size, and its inversion grade is higher. The inversion grade and crystallite size results are in agreement to the tendency predicted by Kamiyama *et al.*[2]

3.4 SEM and EDX

Figure 3 shows the microstructure of 4CM and 6PM samples fired at 900 C/6 h. It can be remarked that a large number of particles are mutually agglomerated indicating a sinterization process

Table 6. Results from EDX analyses of 4 CM, 5 PM and 6 PM samples fired at 900°C/6 h

	wt%		*Nos of ions*		
	Fe_2O_3	*ZnO*	*Fe*	*Zn*	*O*
4CM	63·02	30·98	16·49	7·26	32·00
5PM	66·29	33·71	16·01	7·99	32·00
6PM	66·82	33·18	16·10	7·85	32·00
Theoretical	66·24	33·76	16·00	8·00	32·00

Table 7. Data from Mössbauer experiences of 2CM, 4CM and 6PM samples fired at 900°C/6 h

sample	*IS* ($mm\,s^{-1}$)	*QS* ($mm\,s^{-1}$)	*Heff* (*kOe*)	*G* (%)	*Phase composition*
2CM	0·371	−0·104	520·1	19·2	α-Fe_2O_3
	0·346	0·367	0	80·8	$ZnFe_2O_4$
4CM	0·348	0·348	0	100	$ZnFe_2O_4$
6PM	0·348	0·356	0	100	$ZnFe_2O_4$

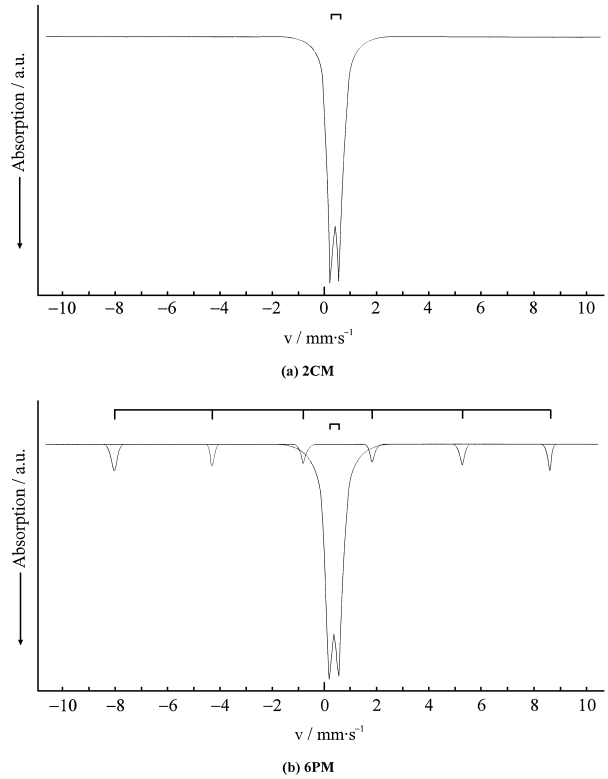

Fig. 4. Mössbauer spectra of (a) 2CM and (b) 6PM samples fired at 900°C/6 h. 4CM sample showed a spectrum identical to 6PM one.

which is more evident in 6PM sample. The ceramic samples presented a higher proportion of particles with irregular shapes than Pechini ones. All Pechini samples showed particles with spherical appearance when they are not agglomerated.

The EDX analyses of samples were carried out with the samples fired at 900°C/6 h to check the quality of samples that have been used to determine structural parameters. The data from EDX analyses (Table 6) indicated that the Fe and Zn content was very similar in all samples, taking into account the resolution and precision of this type of analytical devices, the average values obtained are in good agreement to those of theoretical ones expected for $ZnFe_2O_4$ spinel.

3.5 Mössbauer Spectroscopy

Another parameter that has to be verified, is the oxidation state of iron, in order to interpret the results encountered properly. So as to confirm the

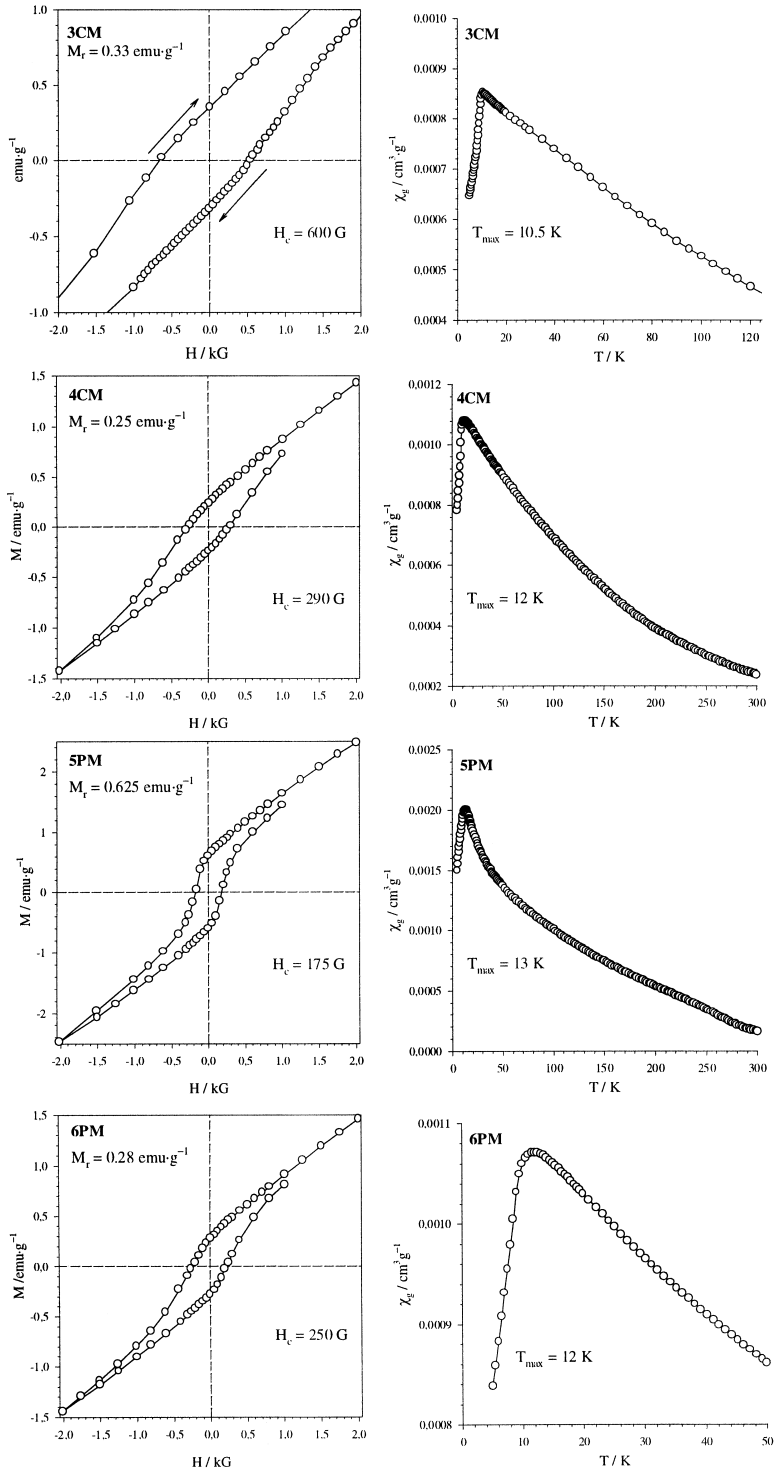

Fig. 5. M–H and χ–T plots of 3CM, 4CM, 7PM and 9PM samples fired at 900°C/6 h. The magnetic hysteresis loop has been taken at 5 K and the χ–T plot has been recorded under a magnetic field of 1000 G.

oxidation state of Fe ions and its distribution over octahedral and tetrahedral positions, Mössbauer spectra at room temperature for 2CM, 4CM and 6PM samples (fired at 900°C, 6 h) were recorded, and the results are shown in Table 7. In Fig. 4, Mössbauer fitted profiles of spectra of 2CM and 6PM fired at 900°C/6 h are shown (experimental points are not drawn for more clarity). The theoretical model of fitting profile used is Lorentzian one. The spectra are highly symmetric, indicating a unique oxidation state for Fe ions. The sharpness of the doublets is also indicative of the fact that iron is unique in its environment and thus homogeneously distributed.[11] The line components are comparatively broad, as one would expect for a randomised distribution, and it is possible to fit one quadrupolar doublet with isomer shifts, IS, appropriate to Fe^{III} ions in high spin coordination over the octahedral sites. The quadrupole splitting values, QS, suggested a high symmetry of the cation sites. The spectrum of 2CM sample is built from two components: a sextet and a quadrupolar doublet, in 4CM and 6PM samples only a quadrupole doublet is detected. The analysis shows that the sextet is close to that observed in α-Fe_2O_3 and it would indicate the presence of Fe_2O_3 in that sample, that was not detected by XRD analysis. Parameters assigned to α-Fe_2O_3 are very close to the ones expected for crystalline hematite.[12] In all samples there is no evidence of Fe^{II} ions. This fact is very important, since the presence of Fe^{II} has an undesirable side-effect associated to the increase of electrical conductivity that could develop eddy current losses[13] which are prejudicial to the electromagnetic properties of these materials.

3.6 Magnetic measurements

The magnetic measurements realised on 3CM, 4CM, 5PM and 6PM samples fired at 900°C/6 h are represented in Fig. 5. The experiences shown in this figure are: magnetic susceptibility χ_g (in $cm^3\,g^{-1}$) versus temperature T (in K) under the presence of a magnetic field of 1000 G; and the magnetisation M (in emu g^{-1}) versus magnetic field H (in kG) at a temperature of 5 K (magnetic hysteresis loop at 5 K). The behaviour of samples is paramagnetic at high temperatures, and antiferromagnetic at temperatures below T_N, as it can be seen in χ–T diagrams. We can observe the variation of the Nëel temperature form theoretical one (10 K) in all samples, which is normally associated to the increasing of interaction forces or to the increasing of the proportion of these stronger interactions. Considering the stoichiometric compositions kept, the evidence of a magnetic hysteresis and the shift of the T_N, we can point out the existence of a certain grade of inversion, which confirms Rietveld analyses results. The 3CM sample shows a very small deviation from theoretical T_N and perhaps for this reason Rietveld analyses cannot detect such a very reduced inversion grade. The 5PM sample presents the greatest deviation from theoretical T_N and its inversion grade is not the greatest one of the group of samples analysed. This non-concordant fact is now under investigation.

4 Conclusions

1. In the ceramic method Fe_2O_3 is not appropriate for obtaining $ZnFe_2O_4$ as a single phase at low temperatures and/or short annealing times.
2. It can be seen (as it is shown in Table 2) that ceramic processing is less reactive than Pechini one, since $ZnFe_2O_4$ appears as a single phase at a minor temperature and with less annealing time. And the best precursors are heptahydrated zinc sulphate as zinc precursor and Mohr salt and heptahydrated iron (II) sulphate as iron precursors.
3. EDX analyses indicate that sample compositions are very close to nominal (theoretical) one. This fact indicate that the synthesis carried out in this study have avoided the reaction of decomposition of the spinel showed in eqn (1).
4. Mössbauer spectra indicate no presence of Fe(II) in any case. This technique is capable of showing Fe(III) associated to α-Fe_2O_3 in such amounts that are not detected in XRD.
5. The results obtained from Rietveld analysis suggest a grade of inversion in the spinel $ZnFe_2O_4$ that is confirmed by the magnetic measurements. These magnetic measurements are actually very sensitive to this 'disordering' in this particular system.

Acknowledgements

The authors would like to express their thanks to Professor Vladimir Kozhukharov from the Higher Institute of Chemical Technology, Sofia University, Bulgaria for his helpful support in obtaining the Mössbauer spectra and its discussions; F. Lloret and M. Julve from the Departamento de Química Inorgánica of Universidad de Valencia for their helpful support in obtaining the magnetic measurements in the SQUID magnetometer and for essential discussions. The research was supported by Fundació Caixa Castelló-Universitat Jaume I, project P1B95-22.

References

1. Schiessl, W., Potzel, W., Karzel, H., Steiner, M., Kalvius, G. M., Martin, M., Krause, K., Halevy, I., Gal, J., Schäfer, W., Will, W., Hillberg, M. and Wäppling, R., Magnetic properties of the $ZnFe_2O_4$ spinel. *Phys. Rev. B*, 1996, **53**(14), 9143–9152.
2. Kamiyama, T., Haneda, K., Sato, T., Ikeda, S. and Asano, H., Cation distribution in $ZnFe_2O_4$ fine particles studied by neutron powder diffraction. *Sol. Stat. Comm.*, 1992, **81**(7), 563–566.
3. Sato, T., Haneda, K., Ijima, T. and Seki, M., In *Ferrites, Proceedings of the ICF6,* ed. by T. Yamaguchi and M. Abe Tokyo, 1992. The Japan Cociety of Powder and Powder Metallurgy, Tokyo, 1992, p. 984.
4. Sato, T., Haneda, K., Seki, M. and Ijima, T., *Proceedings of the International Symposium on the Physics of Magnetic Materials* World Scientific, Singapore, 1987, p. 210–213.
5. Sato, T., Haneda, K., Seki, M. and Ijima, T., Morphology and magnetic properties of ultrafine $ZnFe_2O_4$ particles. *Appl. Phys. A*, 1990, **50**, 13–16.
6. Wold, A., The preparation and characterization of materials. *J. Chem.*, 1980, **57**(8), 531–536.
7. O'Neill, H. St. C., Temperature dependence of the cation distribution in zinc ferrite ($ZnFe_2O_4$) from powder XRD structural refinements. *Eur. J. Mineral*, 1992, **4**, 574–575.
8. Pechini, M., US Patent. 3 330697, 11 July 1967.
9. Gajghiye, N. S., Bhattacharya, U. and Darshane, V. S., Thermal decomposition of zinc–iron citrate precursor. *Thermochimica acta*, 1995, **264**, 219–230.
10. Rodríguez-Carvajal, J., FullProf program, version 3.1, July 1995-LLB-JRC. Laboratoire Leon Brillouin, CEA-CNRS, France.
11. Bhattacharya, A. K., Hartridge, A., Mallick, K. K., Majumdar, C. K., Das, D. and Chintalapudi, S. N., An X-ray diffraction and Mössbauer study of nanocrystalline Fe_2O_3–Cr_2O_3 solid solutions. *J. of Mater. Sci.*, 1997, **32**, 557–560.
12. Greenwood, N. N. and Gibb, T. C.,*Mössbauer Spectroscopy*. Chapman and Hall, London, 1971, p. 241. Chapter 10.
13. West, A. R.,*Solid State Chemistry and Its Applications*. John Wiley and Sons, New York, 1992, pp. 575, 580.